PHYSICAL REVIEW B VOLUME 38, NUMBER 5 15 AUGUST 1988-I

Internal-stress effects on Raman spectra of $In_xGa_{1-x}As$ on InP

Shuichi Emura and Shun-ichi Gonda
The Institute of Scientific and Industrial Research, Osaka University, Mihogaoka, Ibaraki, Osaka 567, Japan

Yūichi Matsui and Hideki Hayashi
Research and Development Group, Sumitomo Electric Industries, Sakaeku, Yokohama, Kanagawa 214, Japan

(Received 13 November 1987)

Raman spectra of $In_xGa_{1-x}As$ are observed over a wide range of composition. A GaAs-like mode frequency ω is found to vary with the composition x as $\omega=-32.4x^2-18.6x+290.0\ \mathrm{cm}^{-1}$. The internal stresses due to lattice mismatch are evaluated from the deviation of the GaAs-like LO mode frequency from the above experimental equation for small lattice mismatch. An increase is found in the internal stress toward the interface from the 5000-Å-thick surface layer. The stress effects on the lattice vibrations of the optical mode are discussed from a microscopic point of view.

I. INTRODUCTION

The ternary alloy semiconductor $In_xGa_{1-x}As$ is a useful material for electronic and optoelectronic devices. As a substrate for $In_xGa_{1-x}As$, InP is often used because of the lattice-matching condition. However, since a lattice mismatch between $In_xGa_{1-x}As$ and InP can occur, it is necessary to investigate the stress or strain in the heterointerface in the case of lattice mismatch. The size of the stress or strain is dependent upon the magnitude of the lattice mismatch and upon the thickness of the epitaxial layers. However, the dependence on these factors, in particular on the latter, has not been elucidated enough. There are several methods for the measurement of stress and strain. Acquisition of information on the lattice vibration by measuring Raman scattering is one of the effective methods.

The lattice vibrations in $In_xGa_{1-x}As$ on InP grown by liquid-phase epitaxy were studied with Raman scattering by Pearsall, Carles, and Portel.[1] They analyzed the polarization properties, and concluded that only one peak of four observed modes displays pure LO-mode behavior, taking into account their magnetophonon resonance results. Early work on infrared reflection by Brodsky and Lucovsky[2] covered the whole range of composition. They found two reflectivity bands and reported the phonon nature in this material as a mixed-mode type with both one- and two-mode phonon. However, it does not seem that the complete assignment of peaks has been established to date. Kakimoto and Katoda[3] measured the Raman spectra from $In_xGa_{1-x}As$ epitaxial layers on InP and GaAs substrates with molar fraction of InAs (x) less than 0.53. They found new Raman peaks from forbidden acoustical and optical modes activated by disorder in the alloy in the middle composition range and observed the broadening of the GaAs-like LO mode due to the stress. However, the stress effects originating with the lattice mismatch were not discussed in detail. The internal stress in epitaxial layers was studied with Raman scattering by several authors[4,5] and experiments under stress were widely performed.[6-8]

In the present paper, Raman spectra of $In_xGa_{1-x}As$ layers on InP substrates are presented over a wide range of composition. The evaluation of the internal stresses of $In_xGa_{1-x}As$ on the InP substrate is made from a shift of the GaAs-like LO-phonon frequency over the range of $|\delta|=(a'-a)/a=0.004$ (where δ is the degree of lattice mismatch, and a' and a are the lattice constants of the $In_xGa_{1-x}As$ layers and of the InP substrate, respectively). The dependence of the Raman spectra on the thickness of the grown layers is also measured by successive etching. The stress effects on the lattice vibrations of the optical mode are discussed from a microscopic point of view.

II. EXPERIMENT

A. Crystal growth

The epitaxial layers were grown by molecular-beam epitaxy on (100) surfaces of Fe-doped, semi-insulating InP substrates ($\rho>10^6\ \Omega\,\mathrm{cm}$). The substrate was chemically etched to remove the damaged surfaces and contaminations with Br_2-CH_3OH solution for 30 sec and then thermally cleaned above 450 °C in enough As_4 atmosphere.

The growth temperature was fixed at 450–500 °C, and the substrate was rotated at 5 rpm during the growth.[9] The growth rate was controlled between 0.24 and 1.32 μm/h by adjusting the flux intensity of group-III elements. In order to eliminate the overshoot of the molecular-beam intensities, which occurred just after opening cell shutters, the shutters were kept apart from the crucibles.[9] The mirrorlike surfaces were obtained for the layers with the lattice mismatch δ within about ± 0.004.

The grown layers were examined with an x-ray double-crystal diffractometer using (400) diffraction. The peaks of the x-ray rocking curve of the epitaxial layers were of almost the same full width at half maximum as the substrate, as shown in Fig. 1(a). This means the good compositional uniformity in the direction of thickness

 ©1988 The American Physical Society

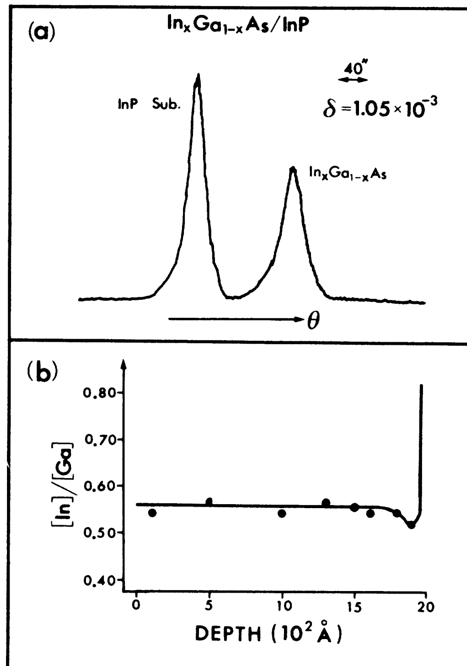

FIG. 1. (a) X-ray rocking curve of $In_xGa_{1-x}As/InP$ by the double-crystal method. The thickness of eptiaxial layer is 0.69 μm. (b) Depth profile of the composition in the direction of crystal growth by Auger-electron-spectroscopy analysis. The composition profile is very flat.

and the good crystalline quality. The degree of lattice mismatch could be evaluated to the value of $\delta=2.0\times10^{-4}$. The variation of composition along the direction of growth was directly checked by Auger electron spectroscopy, using ion sputter etching. The results are shown in Fig. 1(b). The variation of the composition is flat within the error of measurements.

B. Measurements of Raman scattering and sample preparation

Raman spectra were observed by means of the backscattering alignment with a large angle of incidence which was close to the Brewster angle, using a 5145-Å line of an Ar laser. The Ar laser was operated at a power level of 300 mW but the light intensity on the sample decreased to ~100 mW. The diameter of the laser beam was about 40 μm. The scattered light was led to a 1-m double monochrometer and the light was detected by a conventional photon counter. All measurements were made at room temperature.

The samples were treated with an etchant of H_2O-H_3PO_4-H_2O_2 (40:5:1) at 30 °C to evaluate the stress gradient along the direction of growth. The etched thickness was measured with an interference microscope within an error of ±100 Å. The Raman spectra were measured just after the successive etching.

III. RESULTS

Figure 2 shows unanalyzed Raman spectra from $In_xGa_{1-x}As$ on an InP substrate with a lattice mismatch of $\delta=-0.031$, -0.010, $\simeq0.00$, $+0.0078$, and $+0.0152$. The compositions corresponding to δ's are shown in the figure. The sharp band with the highest frequency corresponds to the GaAs-like LO-phonon mode. The four peaks found by Pearsall, Carles, and Portel[1] in their sample with $x=0.53$ are not apparently observed, that is, the lower two bands at 226 cm^{-1} and 244 cm^{-1} are not observed as separate peaks in our samples. In In-rich samples, the lower these bands are not distinguished as distinct peaks. Our analyzed Raman spectra are generally consistent with the results of Pearsall, Carles, and Portel.[1] However, the Raman intensity of the lower three bands in In-rich samples with polarization parallel to that of the incident beam is slightly attenuated, displaying an InAs-like LO mode. It has been reported that $In_xGa_{1-x}As$ alloy displays a two-mode phonon nature involving an InAs-like and a GaAs-like mode.[1–3] Our results of the analyzed Raman spectra from the In-rich samples support that $In_xGa_{1-x}As$ alloy displays a two-mode or a mixed-mode phonon nature.

The peak positions are illustrated in Fig. 3 as a function of the composition x for the samples with $|\delta|$ larger than 0.004 and with $\delta=0.000$. Raman peak positions of the samples with $|\delta|$ less than 0.004 will be shown later in detail to evaluate the internal stresses. The lowest

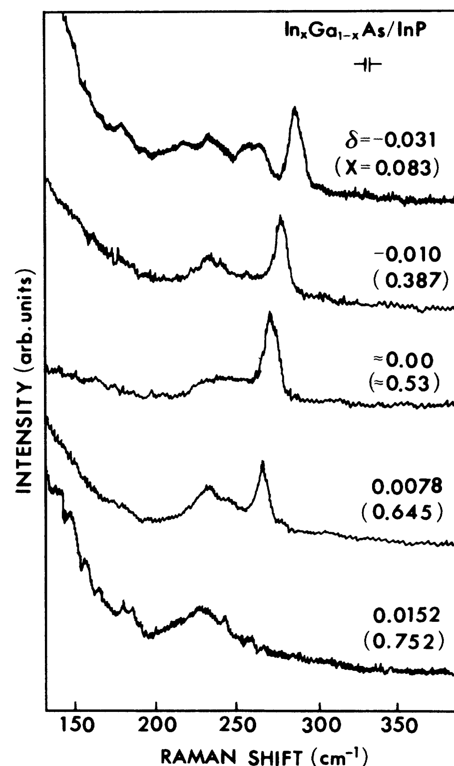

FIG. 2. Unanalyzed Raman scattering spectra from the $In_xGa_{1-x}As$ samples with various δ. The compositions corresponding to δ are shown in the figure.

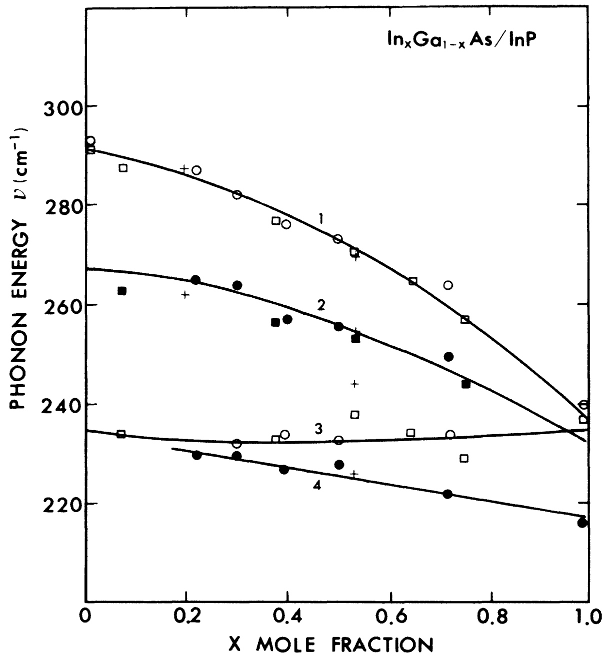

FIG. 3. The composition dependence of Raman-active four modes in $In_xGa_{1-x}As$. □ and ■ show Raman experimental results in this work, + Raman results by Pearsall *et al.* (Ref. 1), and ○ and ● infrared reflectivity results by Brodsky and Lucovsky (Ref. 2). The solid lines indicate the curves calculated using equations derived by least-squares calculation to the second-order polynomial. The numbers attendant to the lines correspond to the equations in the text.

band (band 4) at 226 cm^{-1} which shows the well-defined InAs-like TO behavior[1] does not plainly appear in our spectra, because the TO mode is almost forbidden in our experimental configuration. When the degree of lattice mismatch exceeds a certain value, imperfections such as dislocation take place in the epitaxial layers and then the cell deformations are relieved.[10–12] Consequently, the lattice constant does not change so much. The frequency changes due to the lattice mismatch are also small (a few cm^{-1} at most).

The compositional variation of the Raman-active mode frequency is not linear. By analogy with the band-gap energy in electronic structure of the ternary alloy semiconductors, a bowing parameter can be introduced for the lattice-mode frequencies. A least-squares calculation for the best fit to the experimental results to the second-order term of x gives the following equations for each band,

$$\omega_1 = -32.4x^2 - 18.6x + 290.0 , \quad (1a)$$

$$\omega_2 = -29.0x^2 - 5.3x + 265.1 , \quad (1b)$$

$$\omega_3 = 8.92x^2 - 7.7x + 234.9 , \quad (1c)$$

$$\omega_4 = -16.5x + 233.7 , \quad (1d)$$

where ω_i is the lattice mode frequency of band i in cm^{-1}. The solid lines in Fig. 3 are the curves calculated by these equations.

In highly mismatched samples, the intensity of the scattered light monotonously increases toward the lower frequency. This is caused by roughness of the surface, which is due to the production of a large amount of imperfections such as misfit dislocations. This intensification of the scattered light may be a measure of surface roughness. Since the internal stress relaxes at the dislocations, the following investigation will be focused to the high-quality epitaxial layers with mirrorlike surfaces.

The Raman spectra of $In_xGa_{1-x}As$ layers are observed somewhat differently by each author except for the highest band corresponding to the GaAs-like LO mode. Furthermore, the InAs-like mode is obscure. Therefore, the distinguishable GaAs-like LO mode will be utilized to evaluate the stresses. The frequency shifts of the GaAs-like LO mode of the samples of $|\delta|$ less than 0.004 with mirrorlike surfaces are shown in Fig. 4, standardizing the frequency of the sample lattice matched to the InP substate ($\delta=0$). In this case the layers with nearly the same thickness (1.6 μm) are chosen to avoid the change of stress by the difference of the thickness. The solid line indicates the frequency change of the GaAs-like LO mode due to the compositional change in bulk $In_xGa_{1-x}As$ obtained from the least-squares calculation in Fig. 3. The frequency changes for the epitaxial layers (solid circles in

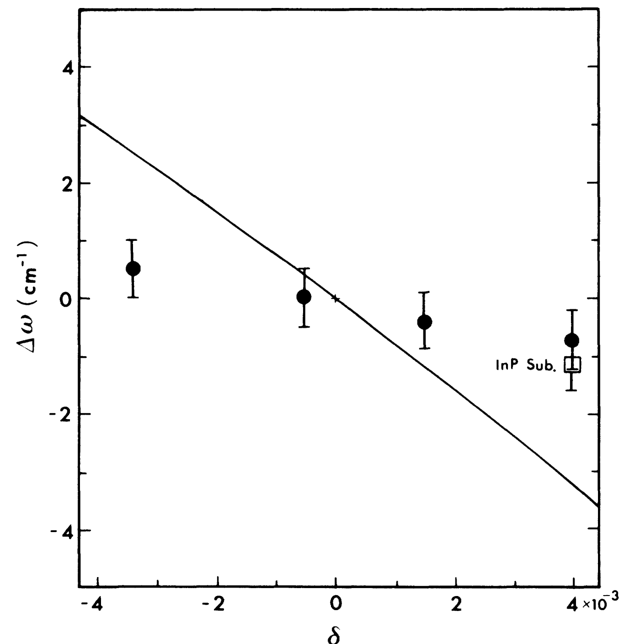

FIG. 4. The frequency shift of the GaAs-like LO mode as a function of the lattice mismatch δ in the range of −0.004 to +0.004. The solid line indicates the compositional change of the GaAs-like LO mode freqeuncy in $In_xGa_{1-x}As$ derived by the least-squares calculation, Eq. (1a), from the experimental values in Fig. 3. The frequency of the lattice-matched composition is standardized because of no internal stresses in this composition. The barred square shows the frequency shift for the InP substrate in the sample with the epitaxial layer thickness of 700 Å. The shift is given as the deviation from the frequency of the bulk InP. The spectrum is depicted in Fig. 6.

Fig. 4) are considerably small, while the frequencies in bulk materials vary by about 6 cm^{-1} from $\delta=-0.004$ to $\delta=+0.004$, which corresponds to composition from $x=0.474$ to $x=0.590$. The deviation from the solid line is considered to be due to the internal stress produced by the lattice mismatch.

The epitaxial layers sustain compression or tension accordingly as the lattice constant of the epitaxial layers is larger ($\delta>0$) or smaller ($\delta<0$) than that of the substrate. The opposite forces may make the antipodal change in the frequency of lattice vibrations. In the case of the GaAs-like LO mode of $In_xGa_{1-x}As$, compression makes the frequency shift higher and tension makes it shift lower, as seen in Fig. 4. This is also true for the relation between the epitaxial layers and the substrate. That is, if the epitaxial layers receive compression, the substrate will sustain tension. These opposite forces for each substance may create the antipodal shifts. This effect is observed in the sample with $\delta=0.004$ and about 700 Å in thickness. The LO mode frequency from the InP substrate of the above sample is shown in Fig. 4, with open squares as the frequency deviation from bulk InP. (The Raman spectrum of the bulk InP is seen in the lower part in Fig. 6). The ratio of the frequency change of the $In_xGa_{1-x}As$ epitaxial layers to that of the InP substrate is about 0.4. This value (smaller than unity) means that the stress coupling is weaker for the LO mode in InP than for the GaAs-like LO mode in $In_xGa_{1-x}As$, because in equilibrium the forces on both sides at the interface must be the same in strength.

It is considered that at the interface between the epitaxial layer and the substrate the strongest stress is produced and that the stress gradually relaxes toward surfaces. It is difficult to measure directly the stress change from the interface to the surface. Here, in order to investigate the outline of the stress change, the change of Raman shift was measured while removing successively the epitaxial layer by chemical etching. The etchant was H_2O-H_3PO_4-H_2O_2 (40:5:1). Since the incident light of wavelength of 5145 Å and the scattered light are strongly absorbed by the epitaxial layers, Raman spectra mainly reflect the lattice vibrations over a range of several hundred Å from the surfaces. The Raman shift $\Delta\omega$ from the frequency of the unetched sample is shown in Fig. 5 as a function of thickness of the etched epitaxial layers. As expected, the largest shifts are observed near the interfaces for both samples. The direction of shift is different following compression or tension. The shifts gradually decrease up to around 5000 Å.

Existence of the stress gradient can also be deduced from unanalyzed Raman spectra drawn in Fig. 6. The lower spectrum shows Raman scattering from the sample etched to about 700 Å with $\delta=0.004$. This spectrum shows the small tail on the higher frequency side of GaAs-like mode as compared with the upper spectrum from the unetched sample. In the case of $\delta>0$, the Raman peaks from the region closer to the interface shift to higher frequency, decreasing the intensity for the strong absorption of the epitaxial layers, if there exists a stress gradient. This should be observed as the tail of band. Therefore, the tail on the higher frequency side of GaAs-like mode is considered to be the evidence for the stress gradient.

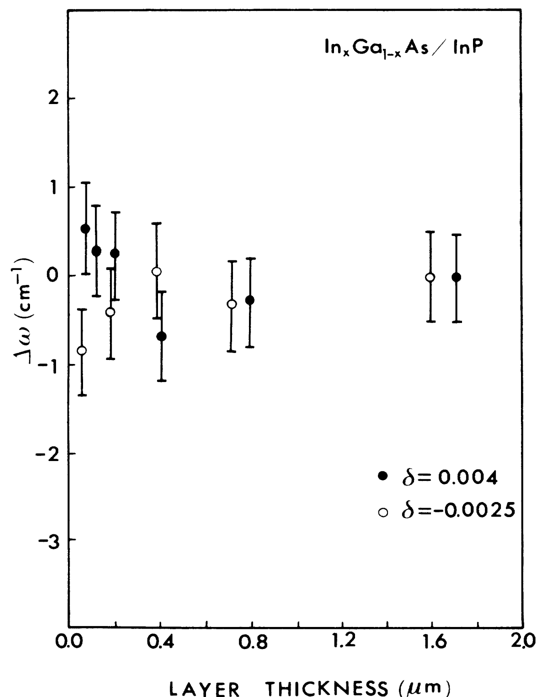

FIG. 5. The frequency shift of the GaAs-like LO mode as a function of the layer thickness for two $In_xGa_{1-x}As$ samples with the different values of δ.

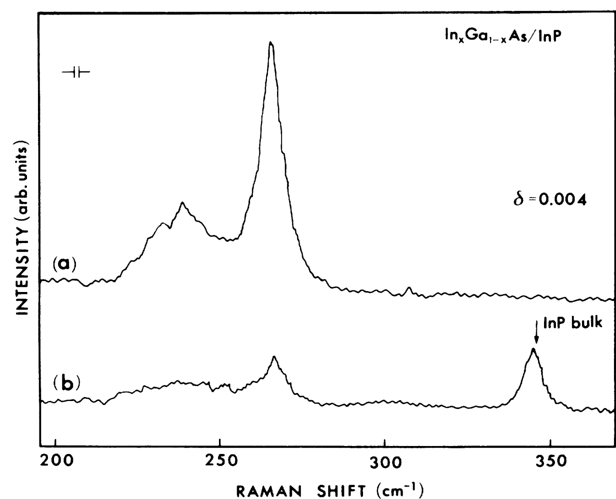

FIG. 6. Unanalyzed Raman spectra from the samples with $\delta=0.004$ and different layer thicknesses: (a) from the thick-enough layer (~ 1.7 μm), (b) from the etched layer to about 700 Å. In (b), the Raman peak from the InP substrate is also observed. This peak slightly shifts to lower frequency. The arrow indicates the peak position of the LO mode in bulk InP.

IV. DISCUSSION

An application of stress (including pressure) to the crystals alters the equilibrium position of the lattice vibrations and also their frequencies. The frequency change is of the second order in coordinates. In this section, we will extend a theory developed by Henry, Schnatterly, and Slichter,[13] and Schnatterly[14] to the second order to analyze the experimental results. Since the total potential depends on the electron and nucleus coordinates, the frequency or the force constant of the optical mode may be treated through an electron-lattice interaction term of the second order in the normal coordinates. The lattice vibrations only at the Γ point in the Brillouin zone are taken into consideration.

Now, the Hamiltonian for an unstressed crystal can be taken at the Γ point as follows:

$$H=H_L(Q)+H_e(\mathbf{r})+H_{eL}(\mathbf{r},Q)$$
$$=H_L(Q)+H_e(\mathbf{r})+\sum_{\nu,\mu} h'_{\nu\mu}(\mathbf{r})Q_{\nu\mu}+\sum_{\substack{\nu,\mu\\ \nu',\mu'}} h''_{\nu\mu}(\mathbf{r})Q_{\nu\mu}Q_{\nu'\mu'} , \quad (2)$$

where H_L and H_e represent the usual Hamiltonians for nuclei and electrons, respectively. Here Q and $\mathbf{r}$ are a normal coordinate for a phonon and an electron coordinate, respectively. $Q_{\nu\mu}$ transforms like the μth basis function of irreducible representation Γ_ν. $H_{eL}(\mathbf{r},Q)$ gives an electron-lattice interaction term to the second order, where $h'_{\nu\mu}$ and $h''_{\nu\mu}$ are quantities depending only on the electron coordinate. A stress term perturbing the other terms,

$$H_s=\sum_{\nu,\mu} F_{\nu\mu}Q_{\nu\mu} , \quad (3)$$

will modify Eq. (2). Here six independent stresses are denoted as $F_{\nu\mu}$. (There are six independent ways of squeezing the crystal.) The components of a symmetric tensor are transformed under cubic symmetry ($\bar{4}3m$) operations as[15–17]

$$\{\Gamma_5\times\Gamma_5\}_s=\Gamma_1+\Gamma_3+\Gamma_5 . \quad (4)$$

Therefore the six stresses $F_{\nu\mu}$ are transformed as the six basis vectors of the irreducible representations Γ_1, Γ_3, and Γ_5.

Then, to the second order in $Q_{\nu\mu}$, we may rewrite Eq. (2) by addition of the term H_s as

$$H=H_L(Q')+H_e(\mathbf{r})+H_{eL}(\mathbf{r},Q')-\sum_{\nu,\mu} h'_{\nu\mu}(\mathbf{r})\Delta Q_{\nu\mu}$$
$$-\sum_{\substack{\nu,\mu\\ \nu',\mu'}} h''_{\nu''\mu''}(\mathbf{r})(2Q_{\nu'\mu'}\Delta Q_{\nu\mu}+\Delta Q_{\nu\mu}\Delta Q_{\nu'\mu'}) , \quad (5)$$

where

$$Q'_{\nu\mu}=Q_{\nu\mu}-\Delta Q_{\nu\mu} , \quad (6)$$

$$\Delta Q_{\nu\mu}=F_{\nu\mu}/M_\nu\omega_\nu^2 . \quad (7)$$

$\Delta Q_{\nu\mu}$ is a strain in the normal coordinate space. The last two terms in Eq. (5) work for the other terms as perturbations separately. The term $h'_{\nu\mu}(\mathbf{r})\Delta Q_{\nu\mu}$ changes the lattice equilibrium position by $\Delta Q_{\nu\mu}$, given by Eq. (7). This results in an electronic perturbation to the lattices. The term $h''_{\nu''\mu''}(\mathbf{r})(2\Delta Q_{\nu\mu}Q_{\nu'\mu'}+\Delta Q_{\nu\mu}\Delta Q_{\nu'\mu'})$ alters the frequency of the phonon. According to the definition of a strain tensor $e_{\nu\mu}$, the last term in Eq. (5) is rewritten as

$$H'(\mathbf{r},Q)=2\sum_{\nu'',\mu''} h''_{\nu''\mu''}(\mathbf{r})\sum_{\substack{\nu,\mu\\ \nu',\mu'}} e_{\nu\mu}Q_{\nu\mu}Q_{\nu'\mu'} . \quad (8)$$

In Eq. (8), the second-order term on $\Delta Q_{\nu\mu}$ is omitted.

In zinc-blende structure constituted with two atoms in a unit cell, there exist two triply degenerate lattice modes in the Γ point which display a symmetry property of an irreducible representation Γ_5. One corresponds to a Raman-active optical mode and the other to an acoustical mode. Then, $\nu=\Gamma_5$ is the relevant normal coordinate. Using a Clebsch-Gordan coefficient, the products $Q_{\nu\mu}Q_{\nu'\mu'}$ are reduced. Thus, the perturbation Hamiltonian to lattice is found in a well-known form by integrating Eq. (8) with the electron coordinate.[18,19] A wave function in the valence band of a III-V alloy semiconductor is transformed as Γ_5 under symmetry operations of a factor group $\bar{4}3m$ in the Γ point. All of the six components of the strain tensor can affect the lattice.

$$H'(Q)=2\{\tfrac{1}{3}Ae_1(\xi\xi+\eta\eta+\zeta\zeta)$$
$$+\tfrac{1}{6}B[e_{3u}(2\zeta\zeta-\xi\xi-\eta\eta)+3e_{3v}(\xi\xi-\eta\eta)]\}$$
$$+\tfrac{1}{2}C[e_{5\xi}(\eta\zeta+\zeta\eta)+e_{5\eta}(\xi\zeta+\zeta\xi)$$
$$+e_{5\zeta}(\xi\eta+\eta\xi)] , \quad (9)$$

where $Q_{5,\kappa}$ ($\kappa=\xi,\eta,\zeta$) is abbreviated as ξ, η, and ζ. Three coupling constants A, B, and C must be determined by experiments.

Now, we can present the perturbation Hamiltonian $H'(Q)$ with stress F. Assuming a linear relation between strains and stresses, the irreducible strain tensors are related to stresses as follows:[20]

$$\begin{aligned} e_1&=e_{xx}+e_{yy}+e_{zz}=-(S_{11}+2S_{12})(\alpha^2+\beta^2+\gamma^2)F ,\\ e_{3u}&=2e_{zz}-e_{xx}-e_{yy}=-(S_{11}-S_{12})(2\gamma^2-\alpha^2-\beta^2)F ,\\ e_{3v}&=e_{xx}-e_{yy}=-(S_{11}-S_{12})(\alpha^2-\beta^2)F ,\\ e_{5\xi}&=e_{yz}=-S_{44}\beta\gamma F ,\\ e_{5\eta}&=e_{zx}=-S_{44}\gamma\alpha F ,\\ e_{5\zeta}&=e_{xy}=-S_{44}\alpha\beta F , \end{aligned} \quad (10)$$

where e_{ij} denotes the strain tensor in Cartesian coordinates, S_{ij} the elastic compliance constant, and α, β and γ direct cosines of stress F to the crystal axes. The z axis is chosen to be perpendicular to the surfaces of the sample. Substituting Eq. (10) for Eq. (9), we can get the Hamiltonian represented with stresses including pressure.

The frequency shift by the stress is given for the optical mode with Γ_5 symmetry as

$$\hbar d\omega=\langle\chi_5(Q)\,|\,H'(Q)\,|\,\chi_5(Q)\rangle , \quad (11)$$

where $\chi_5(Q)$ represents a wave function of a phonon with Γ_5 symmetry. $H'(Q_{\nu\mu})$ not only makes the frequency

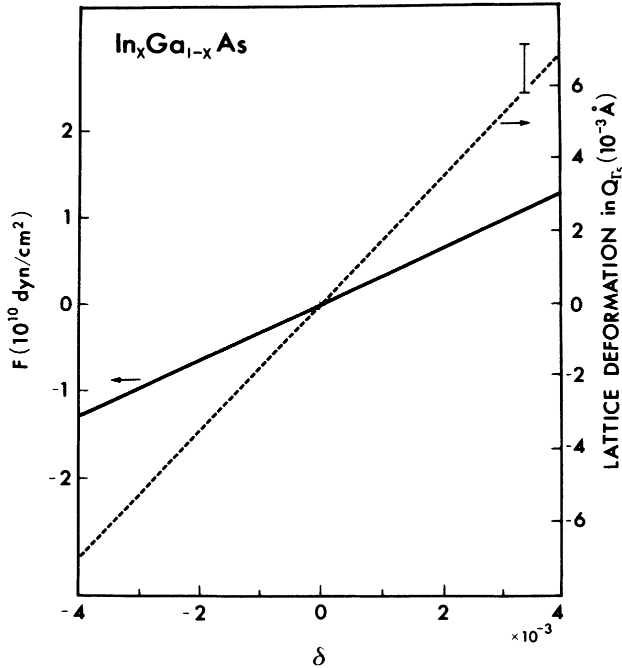

FIG. 7. Internal stress estimated from Eq. (12) (solid line) and lattice deformation $\Gamma_{5,\zeta}$ space from Eq. (13) (dashed line).

shift but also lifts the triply degenerate state of Γ_5. For a biaxial stress along ⟨100⟩ and ⟨010⟩ directions, Eq. (11) is expressed as,

$$\hbar d\omega = 4[-A(S_{11}+2S_{12})\langle \chi_5(Q) \,|\, \xi\xi+\eta\eta+\zeta\zeta \,|\, \chi_5(Q)\rangle + B(S_{11}-S_{12}) \times \langle \chi_5(Q) \,|\, 2\zeta\zeta-\xi\xi-\eta\eta \,|\, \chi_5(Q)\rangle]F \ . \quad (12)$$

So far as we know, no stress experiment is reported on the phonon and elastic properties in the ternary alloy $In_xGa_{1-x}As$. Therefore, we assume that the local values of A, B, and S_{ij} around GaAs molecules in the ternary alloy $In_xGa_{1-x}As$ are almost the same as those of bulk GaAs. That is, using the values from the stress experiment of GaAs by Cerdeira *et al.*[7] for the coupling constants A and B for the GaAs-like LO mode in $In_xGa_{1-x}As$, the internal stresses are evaluated. This is shown in Fig. 7 with a solid line as a function of δ.

This result is considered to be somewhat underestimated from the following reasons. Recent studies by extended x-ray absorption fine structure (EXAFS) on the ternary alloy $In_xGa_{1-x}As$ (Refs. 21–23) have shown that the local surroundings of GaAs in $In_xGa_{1-x}As$ are rather close to the constituent compound GaAs. Even in the dilute limit, the bond length between Ga and As (InAs:Ga) or between In and As (GaAs:In) changes only by one-fifth of the difference between the Ga–As length in GaAs and the In–As length in InAs. However, being not too small, the change will have an effect to increase S_{ij}. Furthermore, the frequency of the GaAs-like mode will soften. This effect also makes S_{ij} increase.

The local deformation $Q_{5,\zeta}$ around GaAs can be estimated from Eq. (7) as a function of δ. Substituting Eq. (10), and the reduced mass of GaAs to Eq. (7),

$$Q_{5,\zeta} = (1.6 \pm 0.2)\delta \ . \quad (13)$$

This result is drawn in Fig. 7 with a dashed line. The positive sign indicates the expansion in the normal coordinate $Q_{5,\zeta}$. The same estimation can be adopted in the deformation of the substrate InP. For the sample with $\delta = 0.004$ and with thickness of 700 Å, we could observe the Raman scattering from the substrate. The deformation of the substrate around the interface is -0.006 Å. This value is nearly the same as that of the epitaxial layer. This result is inevitably reached because of the same strength of the stress on the both side of the interface and the nearly same force constant for the lattice mode in the both substances.

V. SUMMARY

The Raman spectra of $In_xGa_{1-x}As$ epitaxial layers on InP substrate are observed over the wide range of composition. For the clearly distinguishable GaAs-like LO mode, the composition dependence of the phonon frequency is found to be expressed as $\omega_1 = -32.4x^2 - 18.6x + 290.0$, introducing the bowing parameter (the second-order term of composition x) by analogy with the band-gap energy of the electronic structure. On the other bands, the best-fit curves are given using following equations: $\omega_2 = -29.0x^2 - 5.3x + 265.1$ for band 2, $\omega_3 = 8.92x^2 - 7.7x + 234.9$ for band 3, and $\omega_4 = -16.5x + 233.7$ (cm^{-1}) for band 4. The internal stresses are evaluated using the stress shift of the frequency in the GaAs-like LO mode and a microscopic theory considering the electron-lattice interaction to the second order. The deformations of the lattice are also estimated in the space spanning for the LO mode. An increase (or a decrease, which depends on the sign of the lattice mismatch δ) in the frequency shift is found from the layer thickness of 5000 Å toward the interface. For the sample with the lattice mismatch of $+0.004$, the shift at 700 Å in layer thickness is about twice the shift at 5000 Å. This fact implies that just at the interface the strong stresses several times as large as the stresses at a point sufficiently apart from the interfaces in thick layers are produced and that the stresses rapidly relax.

ACKNOWLEDGMENTS

We wish to thank Y. Kishimoto and S. Miyamoto for the assistance in Raman experiments. This work is partially supported by the Agency of Industrial and Science and Technology, Ministry of International Trade and Industry in Japan, in the frame of the Research and Development Project of Basic Technology for Future Industries, "Super-Lattice Devices."

[1]T. P. Pearsall, R. Calres, and J. C. Portel, Appl. Phys. Lett. **42**, 436 (1983).
[2]M. H. Brodsky and G. Lucovsky, Phys. Rev. Lett. **21**, 990 (1968).
[3]K. Kakimoto and T. Katoda, Appl. Phys. Lett. **21**, 826 (1982).
[4]B. Jusserand, P. Voisin, M. Voos, L. L. Cheng, E. E. Mendez, and L. Easaki, Appl. Phys. Lett. **46**, 678 (1984).
[5]F. Cerdeira, A. Pinczuk, J. C. Bean, B. Batlogg, and B. A. Wilson, Appl. Phys. Lett. **45**, 1138 (1984).
[6]E. Anastassakis, A. Pinczuk, and E. Burstein, Solid State Commun. **8**, 133 (1970).
[7]F. Cerdeira, C. J. Buchenauer, Fred H. Pollak, and M. Cardona, Phys. Rev. B **5**, 580 (1972).
[8]S. S. Mitra, O. Brafman, W. B. Baniels, and R. K. Crawford, Phys. Rev. **186**, 942 (1969).
[9]Y. Matsui, H. Hayashi, K. Kikuchi, S. Iguchi, and K. Yoshida, J. Vac. Sci. Technol. B **3**, 528 (1985).
[10]S. Sakai, T. Soga, and M. Umeno, Jpn. J. Appl. Phys. **25**, 1680 (1980).
[11]J. W. Matthews and A. E. Blakeslee, J. Cryst. Growth **27**, 118 (1974).
[12]I. J. Fritz, S. T. Picraux, L. R. Dawson, T. J. Drummond, W. D. Laidig, and N. G. Anderson, Appl. Phys. Lett. **46**, 967 (1985).
[13]C. H. Henry, S. E. Schnatterly, and C. P. Slichter, Phys. Rev. **137**, A583 (1965).
[14]S. E. Schnatterly, Phys. Rev. **140**, A1364 (1965).
[15]J. A. Salthouse and H. J. Ware, *Point Group Character Table and Related Data* (Cambridge University Press, London, 1972).
[16]T. Inui, Y. Tanabe, and Y. Onodera, *Group Theory and Its Applications in Physics* (Syokabo, Tokyo, 1976) (in Japanese).
[17]G. L. Bir and G. E. Pikus, *Symmetry and Strain-Induced Effects in Semiconductors* (Wiley & Sons, New York, 1974) p. 295.
[18]W. Hayes and H. F. MacDonald, Proc. R. Soc. London, Ser. A **297**, 503 (1966).
[19]A. S. Barker, Jr. and A. J. Sievers, Rev. Mod. Phys. **47**, S76 (1975).
[20]W. Gebhardt and K. Maier, Phys. Status Solid **8**, 303 (1965).
[21]J. C. Mikkelsen, Jr. and J. B. Boyce, Phys. Rev. Lett. **49**, 1412 (1982).
[22]J. C. Mikkelsen, Jr. and J. B. Boyce, Phys. Rev. B **28**, 7130 (1983).
[23]C. K. Shih, W. E. Spicer, W. A. Harrison, and A. Sher, Phys. Rev. B **31**, 1139 (1985).